A Multipole Analysis of a Dielectric Loaded Coaxial Rectangular Waveguide

Magdy Z. Mohamed and John M. Jarem, *Member, IEEE*

Abstract—**A multipole analysis of a coaxial rectangular waveguide whose inner conductor is circular is made in order to determine the TE and TM modes of the system. The analysis is based on using multipole (dipole, quadrupole, etc.) electric and magnetic current sources to generate field solutions in the waveguide. These solutions are used to match electromagnetic boundary condition in a homogeneous coaxial rectangular waveguide and determine the TE and TM eigenvalues of the waveguide system. The analysis is a generalization of a method first proposed by Mahmoud and Wait [1] to study propagation along thin wires in a coal mine shaft. Eigenvalue results of the multipole method are compared with results of the Generalized Spectral Domain method [5], [6] and are compared to eigenvalue results of a ridged waveguide [13].**

Propagation in a coaxial rectangular waveguide is also studied when the coaxial rectangular waveguide is loaded with lossy inhomogeneous dielectric material. A variational formula is used to relate the TEM, TE and TM modes of an empty coaxial rectangular waveguide to the propagation in the loaded inhomogeneous dielectric waveguide. Propagation in a four wire anechoic chamber is given as an example of the application of the theory developed in the paper.

I. Introduction

AN INTERESTING problem in the area of electromagnetics is the problem of determining the propagation characteristics of a coaxial rectangular waveguide which is either loaded or not loaded with complex, lossy inhomogeneous, dielectric material. Research on this problem has been worked on by many authors including Mahmoud and Wait [1] who studied the propagation characteristics of a thin wire in a coal mine, Sarkar *et al.* [2], Gruner [3], who studied the propagation characteristics of a coaxial rectangular waveguide (with the application of using the coaxial rectangular waveguide as a communication element in a microwave circuit) and by Heinrich *et al.* [4] (and many other authors) who studied the propagation characteristics of shielded microstrip lines with applications to millimeter and microwave theory. Omar and Schümemann [5], [6] just very recently have developed a generalized spectral domain (GSD) method to determine the eigenmodes of a coaxial waveguide (containing either circular or rectangular conductors).

A further application of the solution for the EM fields and propagation constants of a coaxial rectangular waveguide, concerns the design of a four parallel wire anechoic chamber system [7], [8] where the wires or inner conductors of the system may or may not be thin. This particular system, as its name implies, consists of four parallel wires which are placed in a long rectangular shaped anechoic chamber whose walls are covered with pyramidal absorbers (see Fig. 1). For more details about the chamber design refer to [8]. The four wire system is used to excite near TEM waves which simulate at low frequencies, a uniform plane wave. Because of the symmetries of the above problem, the propagation characteristics of the above system are not changed if one studies an inhomogeneously dielectric loaded coaxial rectangular waveguide which is electrically short circuited on three sides and magnetically short circuited on one side (see Fig. 2).

The purpose of the present paper will be to present an analysis of a coaxial rectangular waveguide when the waveguide is and is not loaded with inhomogeneous dielectric. The numerical analysis will be based on a two part approach. The first part consists of using multipoles to determine the TEM, TE, and TM modes of a homogeneous, coaxial rectangular waveguide. The modes (TEM, TE, and TM) which result from the multipole analysis are then used as trial functions in a variational expression presented by Harrington [9] to define a matrix eigenvalue equation whose solution then gives the propagation constants of the lossy dielectric loaded, coaxial waveguide system.

The method to be presented in this paper will be a generalization of the method first presented by Mahmoud and Wait [1] to solve for the EM fields of a thin wire in a coal mine shaft. The coal mine shaft was modeled as a parallel plate waveguide which is transversely loaded with lossy dielectric material in all parts of the waveguide except the shaft area itself. The basis of their method was to use an electric monopole to excite an EM field solution in an empty waveguide and then use this solution to match EM boundary conditions at the thin wire surface, and thus find the eigenmodes of the coaxial waveguide. The present paper will generalize the MW [1] method by using a series of multipoles (dipoles, quadrupoles, etc.) to generate linear combinations of source excited fields to match EM boundary conditions at the inner coaxial conductor. Use of a linear combination of multipole excited field solutions allows a more accurate matching of EM boundary

Manuscript received February 13, 1991; revised September 11, 1991.

The authors are with the Department of Electrical and Computer Engineering, The University of Alabama in Huntsville, Huntsville, AL 35899.

IEEE Log Number 9105446.

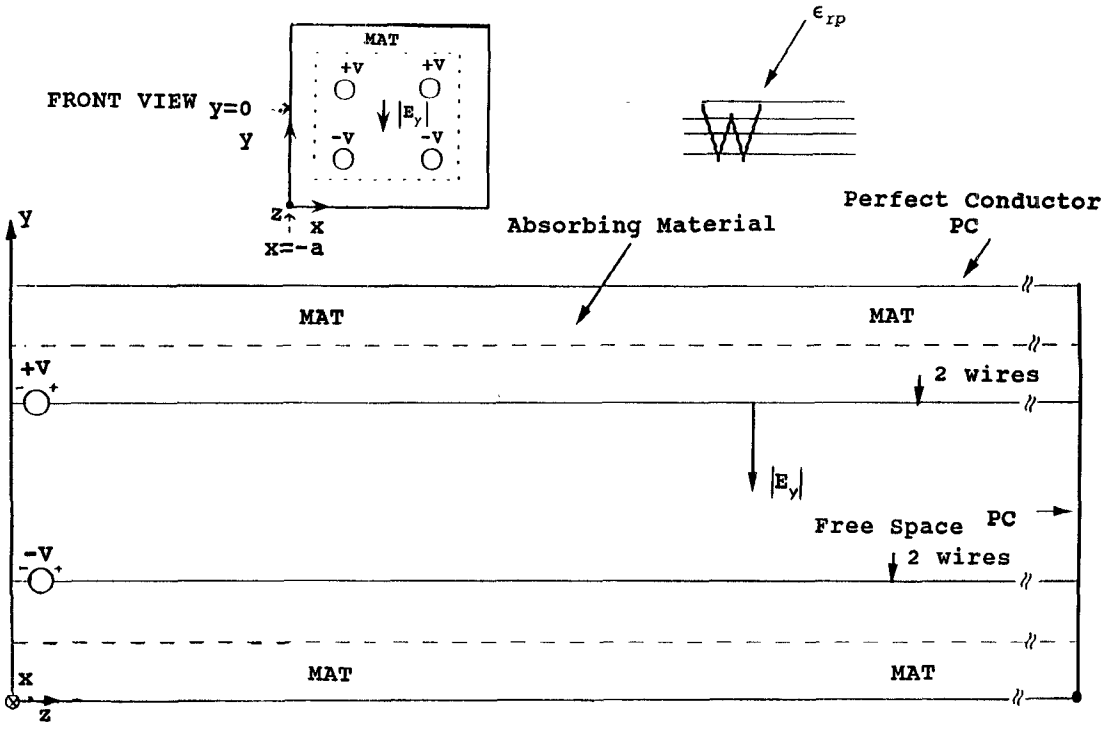

Fig. 1. A simple model of a four wire anechoic chamber is shown. The dielectric layer variation was taken to be $\epsilon_r(N) = 1 - (\epsilon_{rp} - 1)(1 - N/H)^2$ where N is the normal distance from the anechoic chamber wall, H is the height of the pyramid and ϵ_{rp} is the relative dielectric permittivity of the pyramid.

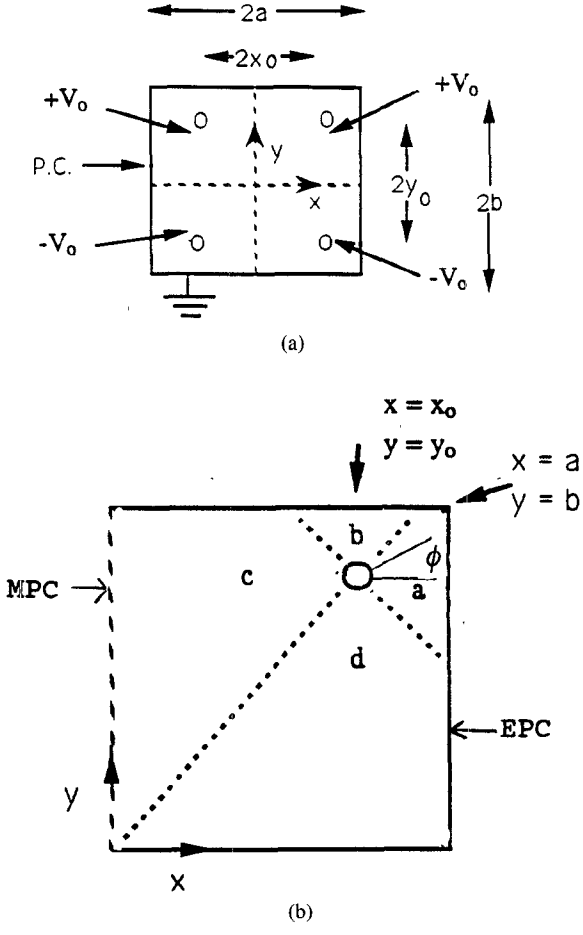

Fig. 2. A cross section of the four wire anechoic chamber is shown in (a) and its wire loaded rectangular waveguide equivalent is shown in (b).

conditions at the inner coaxial conductor than is possible with a single monopole excited field, which thus means that a more accurate determination of the eigenmodes of the system can be made, particularly when the inner coaxial conductor is not small. The generalization of the MW [1] method by use of a series of multipoles is also useful, as it allows eigenmodes in the coaxial guide, as is shown later, to have ϕ azimuthal variation around the inner conductor of the coaxial system (see Fig. 2(b)) rather than just nearly ϕ-independent variation as occurs from a single monopole alone. Earlier research on azimuthal current distribution on circular wires has been worked on by Bridges [10] who studied the interface effects on the propagation constant and fields of a bare conductor buried in a lossy half-space and by Pogorzelski and Chang [11] who studied the validity of the thin wire approximation in analysis of wave propagation along a wire over a ground. A very recent paper by Omar and Schünemann [5] (using GSD) has studied the ϕ azimuthal dependence of the TE and TM modes of a coaxial inner conductor when the inner conductor was circular. The generalized multipole technique is presented by Hafner [12].

In addition to the previously described anechoic chamber example, the theory developed in this paper may be of use to anyone who is interested in studying propagation in shielded microstrips (either with or without inhomogeneous dielectric present) or coaxial waveguides in which the inner conductor radius is or is not small. The theory of this paper will be of interest to these people, because as is well known, the solution of microstrip or coaxial waveguide problems in the inner conductor parameter

range just listed can be quite difficult to solve by finite difference (FD) or finite element (FE) methods. The above problem is difficult to solve by FD and FE methods (particularly for higher order modes) as the inner conductor in the above parameter range causes sharp discontinuities in the EM fields of the waveguide system near the inner conductor, discontinuities, which require prohibitively small grid element spacing (which result in large eigen matrix system) for accurate modeling.

II. Coaxial, Rectangular Waveguide Multipole Solution

The present authors are interested in this section in using the method presented by MW [1] to derive the TE and TM modes of a coaxial rectangular waveguide. Several important remarks about the analysis need to be discussed before the analysis is made. The first remark concerns the fact that if the conductivity of the lossy dielectric material used in [1] approaches infinity, it is found that the resulting eigenvalue equation only predicts the TM modes of the waveguide and cannot predict any TE modes. TE modes would not arise in the formulation of [1] (when $\sigma \rightarrow \infty$), as [1] didn't consider the EM fields that could arise from a magnetic delta source (same as a magnetic monopole source) as they were only interested in propagation modes which were coupled directly to the thin wire. They had assumed that all other modes (including TE modes if $\sigma \rightarrow \infty$) could be determined from the waveguide when the thin wire was not present in the waveguide. For a thin wire system this is a very good approximation. The present investigation is interested in identifying all modes, TEM, TE, and TM, which are coupled to the inner conductor and which can propagate in the rectangular waveguide. We are interested in this case as here we are not necessarily assuming that the inner conductor is thin.

A second remark that should be stated is the fact that as $\sigma \rightarrow \infty$, the potentials of [1] reduce to and are equivalent to using a magnetic vector potential $\vec{A} = A_z \hat{a}_z$ in the waveguide. This vector potential will be used to determine TM modes in the present problem. The vector potential $\vec{F} = F_z \hat{a}_z$ will determine the TE modes.

A third remark that should be made concerning the derivation of TE and TM modes in a coaxial waveguide using the method of MW [1] concerns the behavior of the azimuthal delta source EM fields when they are evaluated arbitrarily close to monopole (delta source) location. For example let us consider the case where the waveguide walls are perfectly conducting and we find the TM fields from $\vec{A} = A_z \hat{a}_z$ using an electric monopole excitation. In examining this solution in free space we can show from the wave equation that the solution arbitrarily close to the monopole acts like a Bessel function of order zero [9, pp. 223–228], and thus has no azimuthal variation. We expect any modal variation of the TM mode near the inner conductor surface to be nearly that of the monopole as the inner conductor radius becomes smaller and approaches zero. If this statement is true, this then means that by using only a single monopole it is not possible to calculate any TM mode which has a nonzero azimuthal variation close to the inner conductor. To illustrate this point a single monopole has been used in the Appendix to calculate the TM modes of a centered, circular coaxial waveguide. The result of the analysis was the eigenvalue equation (A7) which is just the eigenvalue equation for $n = 0$ (ϕ independent) coaxial circular waveguide modes. For the case of a centered circular coaxial waveguide use of a single monopole, could not identify all of the other $\{\cos n\phi, \sin n\phi\}$ eigensolutions known to exist in a coaxial circular waveguide.

The present authors believe that a way to solve for TE or TM modes that do have a nonzero azimuthal variation about the inner conductor is to use multipoles (or linear combinations of them) as described in [9, pp. 223–228] to excite the homogeneous fields in the system which are to be used to match EM boundary conditions at the inner conductor surface. The multipoles as described in [9] consist of electric and magnetic dipoles, quadrupoles, etc., with each of the individual monopoles separated from one another by a small distance Δs which is assumed in the limit to go to zero. As shown in [9] the field solutions of the higher order derivative multipoles in free space vary sinusoidally around the multipole line sources. In the rectangular waveguide, the same property can be expected to hold at least approximately when the fields are evaluated close to the multipoles. Because the multipole field responses do vary approximately sinusoidally in ϕ (see Fig. 2(b)) near the multipole sources, the linear combinations of the multipoles in this paper will be chosen in such a way as to form (at least approximately) a Fourier series in the coordinate ϕ around the inner conductor. The latter part of the Appendix shows how this method can be used to determine, for example, the TE_{11} mode ($F_z = J_1(k_T r) \sin \phi$) of a centered circular coaxial waveguide.

The assumption that a set of multipoles will lead to a sinusoidal variation of the fields in the azimuthal coordinate ϕ around the multipoles is justified by the fact, that very close to the multipoles, the wave equation for A_z which is given by

$$\begin{aligned}\nabla_t^2 A_z + k_T^2 A_z = {} & -I_o\, \delta(x - x_o)\, \delta(y - y_o) \\ & - I_{1x}\left[\delta(y - y_o)\left[\delta\left(x - x_o - \frac{\Delta s_x}{2}\right)\right.\right. \\ & \left.\left. - \delta\left(x - x_o + \frac{\Delta s_x}{2}\right)\right]\right] \\ & - I_{1y}\left[\delta(x - x_o)\left[\delta\left(y - y_o - \frac{\Delta s_y}{2}\right)\right.\right. \\ & \left.\left. - \delta\left(y - y_o + \frac{\Delta s_y}{2}\right)\right]\right] \\ & + \cdots \text{ higher order terms} \end{aligned} \tag{1}$$

when it is driven by a series of multipoles, can be very well approximated by dropping the $k_T^2 A_z$ term in the above equation and solving Poisson's equation (with free space boundary condition) to get an accurate near field solution. If in (1), for example, we keep only the I_{1y} term, the solution for A_z becomes the well known electrostatic dipole solution:

$$A_z = \frac{I_{1y}\Delta s_y}{2\pi r}\sin\phi \tag{2}$$

As can be seen, a $\sin\phi$ variation occurs when a first order multipole is used. A discussion of electrostatic multipoles may be found in Hafner [12] and Jackson [13].

The procedure for calculating the multipole field response consists of simply calculating the delta response of a single monopole in a rectangular waveguide, and then differentiating this delta function response with the operator $(\partial^m/\partial x_o^m)(\partial^n/\partial y_o^n)$ where x_o and y_o are the source coordinates of the delta source. As shown in [9] the multipole responses which have been formed by differentiation by the $\partial/\partial x_o$ and $\partial/\partial y_o$ operators will have associated with them in all of free space, respectively, a $\cos\phi$ and $\sin\phi$ variation. From this information one can conclude that the multipole response formed from a $(\partial^m/\partial x_o^m)(\partial^n/\partial y_o^n)$ differentiation will have a multipole response which has a $\cos^m\phi\sin^n\phi$ variation associated with it. By choosing the proper linear combinations of $\{\cos^m\phi\sin^n\phi\}$ $m = 0, 1, 2, \cdots; n = 0, 1, 2, \cdots$ it is possible in free space to construct a linear combination of the multipole responses so that its response equals $\cos(l\phi)$ or $\sin(l\phi)$, $l = 0, 1, 2 \cdots$. In a waveguide by analogy with the free space case, the linear combinations of multipoles in free space which produced the $\cos(l\phi)$, $\sin(l\phi)$ variation will produce in the waveguide, near the inner conductor, a linear combination of multipole responses which have a ϕ variation which is not precisely a $\cos(l\phi)$ or $\sin(l\phi)$ function, but one which approximately equals this variation. (See Fig. 5 for a numerical example.) These near sinusoidal multipole responses (near to $\cos(l\phi)$ or $\sin(l\phi)$) can be used to form a series in ϕ which is close to being a sinusoidal Fourier series and thus a very useful one with which to expand and determine the unknown EM fields which exist near the inner conductor surface.

Based on the preceding discussion, the procedure that has been used to calculate the TE and TM modes of the waveguide system consists of expanding the unknown EM fields near the inner conductor surface in the near sinusoidal Fourier series (with as yet still unknown coefficients) which has been described in the previous paragraph and then forcing the tangential electric field associated with this series to be zero at the inner conductor surface to meet EM boundary conditions. Sinusoidal testing functions are used to impose the just described EM boundary condition (see (9)). Concerning the numerics of the proposed procedure, we may say that the closer that the near Fourier series described in the previous paragraph is to an exact Fourier series in ϕ, the closer then is the present procedure to being an orthonormal one (and therefore a highly desirable one which produces a diagonal matrix eigenvalue equation) since in this case sinusoidal terms are being used for both expansion and testing functions at the inner conductor surface. When the near Fourier series deviates from a sinusoidal series at the inner conductor surface, the testing and expansion procedure, becomes a non-Galerkin one, but is still nevertheless a valid procedure for eigenmode determination of the system.

To illustrate the procedure, we will present the formulation of the TE case when three waveguide walls are perfect electric conductors and one wall is a perfect magnetic conductor (see Fig. 2(b)). The electric vector potential response of a delta magnetic source of strength $K_o\,\delta(x - x_o)\,\delta(y - y_o)$ which excites the wave equation at cutoff:

$$[\nabla_t^2 + k_T^2]F_z = -K_o\,\delta(x - x_o)\,\delta(y - y_o) \tag{3}$$

is given by

$$F_z^{(a)} = \sum_{n=0}^{\infty} \underline{F}_{zn}^{(a)} \cos k_{xn}(x - a)\cos\frac{n\pi}{b}y$$

$$F_z^{(b)} = \sum_{m=0}^{\infty} \underline{F}_{zm}^{(b)} \sin\left(m + \frac{1}{2}\right)\frac{\pi}{a}x\cos k_{ym}(y - b)$$

$$F_z^{(c)} = \sum_{n=0}^{\infty} \underline{F}_{zn}^{(c)} \sin k_{xn}x\cos\frac{n\pi}{b}y$$

$$F_z^{(d)} = \sum_{m=0}^{\infty} \underline{F}_{zm}^{(d)} \sin\left(m + \frac{1}{2}\right)\frac{\pi}{a}x\cos k_{ym}y \tag{4}$$

where

$$\underline{F}_{zm}^{(i)} = X_m \sin\left(m + \frac{1}{2}\right)\frac{\pi}{a}x_o \begin{cases} \cos k_{ym}(y_o - b), & i = d \\ \cos k_{ym}y_o, & i = b \end{cases}$$

$$\underline{F}_{zn}^{(i)} = Y_n \cos\frac{n\pi}{b}y_o \begin{cases} \cos k_{xn}(x_o - a), & i = c \\ \sin k_{xn}x_o, & i = a \end{cases}$$

$$X_m = \frac{-K_o}{\frac{a}{2}k_{ym}\sin k_{ym}b},$$

$$Y_n = \frac{K_o}{(1 + \delta_{o,n})\frac{b}{2}k_{xn}\cos k_{xn}a}$$

$$k_{xn} = \begin{cases} \sqrt{k_T^2 - \left(\frac{n\pi}{b}\right)^2}, & k_T > \frac{n\pi}{b} \\ -j\sqrt{\left(\frac{n\pi}{b}\right)^2 - k_T^2}, & k_T < \frac{n\pi}{b} \end{cases}$$

$$k_{ym} = \begin{cases} \sqrt{k_T^2 - \left(\left(m + \frac{1}{2}\right)\frac{\pi}{a}\right)^2}, \\ \qquad k_T > \left(m + \frac{1}{2}\right)\frac{\pi}{a} \\ -j\sqrt{\left(\left(m + \frac{1}{2}\right)\frac{\pi}{a}\right)^2 - k_T^2}, \\ \qquad k_T < \left(m + \frac{1}{2}\right)\frac{\pi}{a}, \end{cases}$$

K_o = strength of the electric delta current source and $\delta_{o,n}$ is the discrete Kronecker delta function. In the above expressions k_T is the unknown eigenvalue of the mode to be determined, and $F_z^{(a)}$, $F_z^{(b)}$, $F_z^{(c)}$ and $F_z^{(d)}$ are the delta function responses to $K_o\,\delta(x - x_o)\,\delta(y - y_o)$ as occur in the regions a, b, c and d of Fig. 2(b). Note that all $F_z^{(i)}$ solutions meet EM boundary conditions at the outer waveguide walls and satisfy (3). It is further important to realize that the $F_z^{(a)}$, $F_z^{(c)}$ functions and the $F_z^{(b)}$, $F_z^{(d)}$ functions are each by themselves full separate solutions of (3) over the entire cross-section of the waveguide. The $F_z^{(i)}$ solutions overlap between adjacent regions. The $F_z^{(a)}$ and $F_z^{(c)}$ converge most rapidly in Regions (a) and (c) of Fig. 2(b) and the $F_z^{(b)}$ and $F_z^{(d)}$ converge most rapidly in Regions (b) and (d) of Fig. 2(b). This is computationally very important when matching EM boundary conditions when the inner conductor is not too large. The solution method of (3) is given in Collin [14].

When all four walls are electric perfect conductors, $F_z^{(a)}$ is given by

$$F_z^{(a)} = \frac{-K_o}{(1 + \delta_{o,n})\frac{b}{2}k_{xn}\sin k_{xn}a} \cos\frac{n\pi}{b}y_o \cdot \cos k_{xn}x_o \cos k_{xn}(x - a)\cos\frac{n\pi}{b}y \quad (5)$$

$F_z^{(c)}$ may be obtained from $F_z^{(a)}$ of (5) by replacing x_o and $(x - a)$ in (5) with $(x_o - a)$ and x, respectively. Further $F_z^{(b,d)}$ may be determined from $F_z^{(a,c)}$ of (5) by reversing x, y and a, b in (5) in an obvious way.

The TE modes of the coaxial rectangular waveguide are derived by writing the F_{zD} vector potential of the coaxial waveguide (D in the subscript is for derivatives) as a linear combination (involving unknown coefficients) of the homogeneous functions which are the responses of the higher order derivative multipoles, and then using this series to match EM boundary conditions at the inner conductor surface. The $F_{zD}^{(i)}$ series is given in any of the four regions a, b, c, and d by the series

$$F_{zD}^{(i)} = \sum_{l=1}^{\infty} a_l L_l F_z^{(i)} = \sum_{l=1}^{\infty} a_l \sum_{p=0}^{\infty} L_l\left(\frac{\partial}{\partial x_o}, \frac{\partial}{\partial y_o}\right) f_p^{(i)}(x_o, y_o)\,\xi_p^{(i)}(x)\,\psi_p^{(i)}(y) \qquad i = a, b, c, d \quad (6)$$

where $p = m$ or n, $\xi_p^{(i)}(x)$ and $\psi_p^{(i)}(y)$ are the x and y sinusoidal modal functions of regions a, b, c or d in (4) (or (5)), $f_p^{(i)}(x_o, y_o)$ are the coefficients of series in (4) (or (5)) for each of the regions $i = a, b, c, d$, L_l is a higher order derivative operator which operates on the coefficients $f_p^{(i)}(x_o, y_o)$, and a_l are unknown coefficients which are to be determined from matching EM boundary condition at the inner conductor surface. The first five L_l derivatives which are used in this paper are given by

$$L_l|_{l=1}^{5} = \left[1, \frac{\partial}{\partial x_o}, \frac{\partial}{\partial y_o}, \frac{\partial^2}{\partial x_o^2} - \frac{\partial^2}{\partial y_o^2}, \frac{\partial^2}{\partial x_o \partial y_o}\right]. \quad (7)$$

These functions, for an inner conductor radius which is not too large, give rise to an axial ϕ variation around the conductor surface of [1, cos ϕ, sin ϕ, cos 2ϕ, and sin 2ϕ].

To match boundary conditions at the inner conductor surface, the $F_{zD}^{(i)}$ series as given by (6) is used to calculate the E_ϕ electric field at the inner conductor surface, and the E_ϕ field, since it is the tangential electric field, is set to zero at the inner conductor surface. The E_ϕ boundary condition is imposed by multiplying the E_ϕ field by the testing functions $\{t_{l'}\}_{l'=1}^{5} = \{1, \cos\phi, \sin\phi, \cos 2\phi, \sin 2\phi\}$. As can be seen from the preceding discussion, the testing and expansion functions form a Galerkin and nearly orthonormal procedure for enforcing EM boundary conditions at the inner conductor surface when the multipole series of (6) is close to a sinusoidal Fourier series. The equations that result from the above procedure are

$$0 = \int_0^{2\pi} t_{l'}(\phi)\,E_\phi(r, \phi)|_{r=\rho}\,d\phi \quad (8)$$

$$0 = \sum_{i=a}^{d} \int_{\phi_i^-}^{\phi_i^+} t_{l'}(\phi)[-\sin\phi E_x^{(i)} + \cos\phi E_y^{(i)}]\,d\phi \quad (9)$$

where

$$E_x^{(i)} = -\frac{\partial F_{zD}^{(i)}}{\partial y}, \quad E_y^{(i)} = \frac{\partial F_{zD}^{(i)}}{\partial x}, \qquad i = a, b, c, d \quad (10)$$

and where

$$\phi_i^- = \left[-\frac{\pi}{4}, \frac{\pi}{4}, \frac{3\pi}{4}, \frac{5\pi}{4}\right]$$

and ϕ_i^+ are $\pi/2$ greater than ϕ_i^-. Substitution of (6) into (8)–(10) leads to a 5×5 matrix equation which can be used to calculate the unknown eigenvalue k_T of the system, calculate the unknown a_l coefficients and thus form the associated TE eigenfunctions of the system. A similar procedure to that which just has been presented for TE modes can be used to calculate TM modes. The procedure can be extended to any number of Fourier terms.

In addition to determining the TE and TM modes of a coaxial rectangular waveguide, it is also necessary, because the coaxial waveguide is a two conductor system, to determine the TEM wave mode which can propagate in the waveguide system in order that a complete field description be known. The TEM wave mode solution in this paper has been determined from a solution of La-

place's equation with boundary conditions appropriate to that of a coaxial waveguide. This solution has been determined in a previous research paper and the details are given [8].

The present method can be applied to shielded microstrip waveguides and coaxial rectangular waveguides where the inner conductor is not necessarily circular if the testing surface shape given in Fig. 2(b) is simply taken to be near that of the noncircular coaxial waveguide inner conductor. In the case of microstrip inner conductor (which is an important example) this shape could be a wide flat rectangle strip or a flattened ellipse of high eccentricity which approximates the shape of the rectangular strip. In applying the method for an arbitrarily shaped inner conductor for TM modes, one would simply evaluate the EM field (E_z or A_z) at the testing surface. In the case of TE modes for an arbitrarily shaped inner conductor, one would have to compute from the transverse electric field E_x and E_y, its tangential component at the surface of the conductor and then set this field to zero at the inner conductor surface. An elliptic shape is suggested to represent a flat strip, as this would avoid the problems of near field edge effects as are known to occur at sharp edges of the strip [5].

III. Circular Insert, TE Waveguide Mode (EPC Walls)—Numerical Results

In order to demonstrate the validity of the present formulation the cutoff wavenumbers and field distribution of the lowest order TE mode in a circular insert loaded rectangular waveguide (4 walls are electrical perfect conductor (EPC)) has been analyzed for two different numerical examples.

The first example consists of determining the two lowest order TE modes of a circular insert loaded rectangular waveguide when the circular insert has a relatively large radius $\rho = .2259$ m and is placed in the center of a rectangular waveguide where $a = 1.001$ m and $b = 1.$ m (see Fig. 3). The two lowest order modes are very nearly degenerate and have nulls in the H_z (H_z is proportional to the F_{zD} field of (6)) magnetic field which occur respectively at the lines $x = a/2$ and $y = b/2$ and have nulls in the electric field which occur respectively at the lines $y = b/2$ and $a/2$. The two lowest order TE modes were found to have cutoff frequencies of $k_T = 2.490085$ m^{-1} and $k_T = 2.492970$ m^{-1}. Despite the closeness in values of the cutoff frequencies, no numerical problem occurred in determining these values. Fig. 3(a) shows the H_z (or F_{zD}) field of the lowest order mode and Fig. 3(b) shows E_ϕ associated with this mode. As can be seen E_ϕ meets EM boundary conditions at the inner conductor surface almost exactly. The other nearly degenerate mode is not shown, but is very similar to that of Fig. 3(a) except that its H_z variation is in the y direction rather than the x direction of Fig. 3(a). Because $a > b$ this is to be expected. An extremely interesting feature of the solution was the fact that for the lowest order mode, only the a_2 coefficient

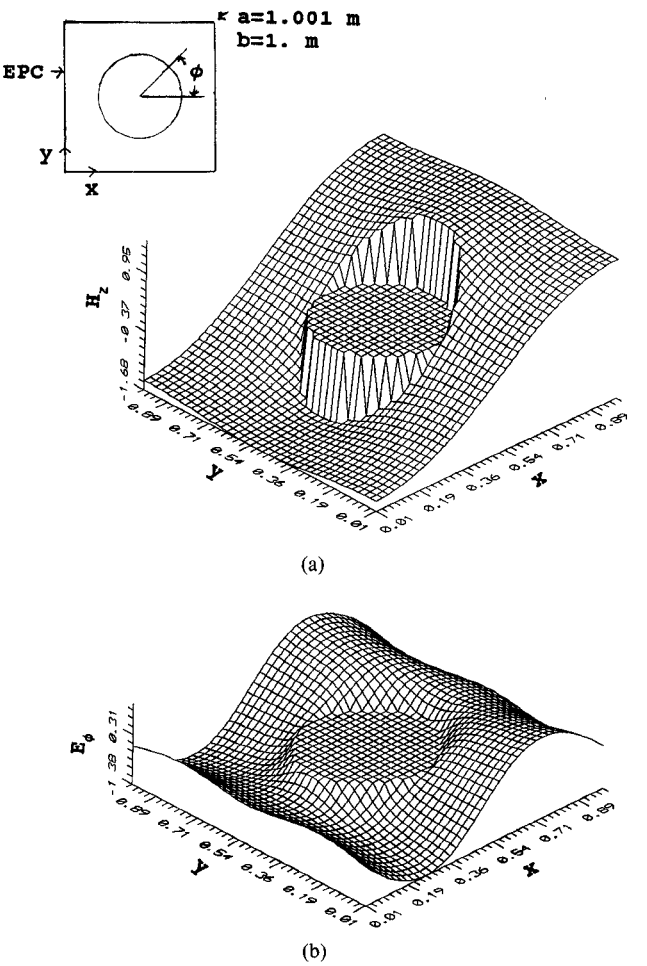

Fig. 3. (a) Shows the H_z field when all four walls are EPC and a centered circular insert of radius $\rho = .2259$ m is placed at the center of the waveguide $a = 1.001$ m and $b = 1.$ m. (b) Shows the E_ϕ electric field over the entire cross section of the guide. The flat circular region shows where the EM fields are zero in the circular insert conductor. (They have been set to zero there.)

($L_2F_z \approx \cos\phi$) of (6) was nonzero (all other coefficients were almost exactly zero). This means that for this case, the L_2F_z multipole was able to exactly provide the eigenmode equation of the waveguide by itself. This occurred despite the large radius used. The same feature occurred for the next higher, almost degenerate mode, except that the a_3 coefficient was nonzero and all of the other coefficients were a zero. The Appendix shows that the L_2F_z multipole provides the exact eigenvalue equation for a circular coaxial waveguide system. It is interesting that when a circular insert is placed in a nearly square rectangular waveguide that the L_2F_z multipole also in this case provides almost the exact eigenvalue equation for the system.

The symmetry of the lowest order TE mode is identical to that of a ridged waveguide which has a circular ridge and occupies 1/4 of the area of the present waveguide system. This is useful as the ridged waveguide results of Utsumi [16, Fig. 3, TE_{10} hybrid mode curves] can be compared approximately to the present results provided that the circular insert areas of the present case and those of Utsumi are made equivalent in value. The value of ρ

= .2259 m in the present example corresponds to the values of $t/a_R = s/b_R = .4$ of Utsumi's paper (a_R and b_R are Utsumi's waveguide dimensions). The cutoff frequency of the ridged waveguide [16] was $k_T = 2.387\ \mathrm{m}^{-1}$ as opposed to $2.490\ \mathrm{m}^{-1}$ for the present case. An unloaded TE_{10} waveguide mode cutoff wavenumber for comparison is $\pi/a = 3.14159\ \mathrm{m}^{-1}$. The agreement is reasonably close considering that Utsumi [16] analyzed a square ridge rather than a circular one.

As a second example, the lowest order TE mode of a rectangular waveguide which has been loaded with a noncentered circular insert has been calculated. The cutoff wavenumber and the TE field distribution has been calculated by two different methods, namely the formulation as given by (5)–(10) of this paper and has been calculated by the Generalized Spectral Domain method as given by [5, Eqs. 1–5]. The rectangular waveguide has been taken to have dimensions $a = 1.001$ m, $b = .85$ m and to be loaded with a circular insert whose radius is .08 m and whose center location is $x_o = .56$ m and $y_o = .62$ m. The insert radius in this example is relatively small and should only perturb the unloaded TE waveguide by a small amount. The GSD solution was calculated by using 11 basis functions of [5, Eq. (2)] namely $\{\cos(i\phi), \sin(i\phi)\ i = 0, 5\}$. Odd and even expansion terms were needed because of the off center position of the insert. The rectangular waveguide modal series of [5, Eq. (1)] includes in its calculation terms up to values of $n = 60$ and $m = 60$. In programming the GSD method [5] all matrix integrals were calculated exactly using Bessel functions and were cross checked by direct numerical integration. Fig. 4(a) shows the H_z field distribution as results from the GSD solution [5], ($k_T = 3.200\ \mathrm{m}^{-1}$) and Fig. 4(b) shows the H_z field distribution as results from Eqs. (5)–(10) of this paper ($k_T = 2.9987\ \mathrm{m}^{-1}$). The H_z field has been set to zero at the flat surface in Figs. 4(a) and (b). As can be seen there is general agreement between the methods with both methods showing that circular insert loaded mode is only slightly perturbed from its unloaded waveguide field distribution. It can also be seen that the GSD method converged well everywhere except close to the insert (the poor convergence or Gibb's phenomenon associated with the GSD method near the wire is discussed in length in [5], [6]) and along a strip near the wire at $y = .62$ m. The multipole method converged extremely smoothly in all parts of waveguide including near the insert surface. Fig. 4(c) show the E_ϕ tangential field component as results from the multipole method. The flat surface in Fig. 4(c) represents the surface where $E_\phi = 0$. The EM boundary condition that the tangential electric field be zero at the surface of a perfect conductor is being satisfied very well. The E_ϕ tangential field using GSD [5, Eq. (3)] was not found to be zero near the wires surface. A disturbing feature of the GSD solution was the fact that the GSD method found a cutoff frequency which was $k_T = 3.2000\ \mathrm{m}^{-1} > \pi/a$ whereas the multipole method found a root where $k_T = 2.999\ \mathrm{m}^{-1} < \pi/a$. The ridged solution of Utsumi [16] indicates that the TE_{10} ridged waveguide mode which corresponds at least approximately to the present case should have a value which is less than π/a. Based on [16] the present authors believe that the eigenvalue of the present example should be less than π/a and close to the value predicted by the multipole method.

Fig. 5(a) and (b) show plots of the individual multipole terms verses the angle ϕ as occurs when the individual multipole terms are evaluated at the surface of the circular insert. Fig. 5(a) shows the L_2F_z term by itself and Fig. 5(b) shows the L_1F_z, L_3F_z, L_4F_z and L_5F_z terms. The L_2F_z was shown alone as it was so much larger than the other terms. As can be seen from the figures the L_3F_z, L_4F_z, L_5F_z terms came remarkably close to being proportional respectively to the sinusoidal terms $\sin\phi$, $\cos 2\phi$ and $\sin 2\phi$ which they were predicted to be by the discussion of (1), whereas the L_1F_z and L_2F_z terms were approximately equal (within 20%) to the sinusoidal terms $\cos 0\phi$ and $\cos\phi$ respectively. Fig. 5(a) and (b) show that the multipole field response provides a basis near the circular insert which although not perfectly sinusoidal, is still nevertheless a highly linearly independent, smoothly varying and well behaved set of basis functions with which to expand the H_z and E_ϕ fields at the surface of the circular insert and thus determine the modes of the system. The fact that the L_2F_z term was large and the other terms small show that the eigen solution converged very quickly to the solution.

In concluding this section it's extremely interesting to note that despite the fact that two different series namely $F_{zD}^{(a)}$, $F_{zD}^{(c)}$ and $F_{zD}^{(b)}$, $F_{zD}^{(d)}$ were used to calculate the fields of Figs. 3(a), 3(b), 4(b), 4(c), 5(a), and 5(b) that no discontinuities from the series solutions can be seen at the Region a, b, c, or d boundaries. The lack of discontinuities in the E_ϕ field shown in Figs. 3(b) and 4(c) is particularly interesting since to calculate this field it was necessary to take partial derivatives of F_{zD} ((6)) with respect to x and y.

IV. Lossy Dielectric Wire Loaded Waveguide

This section will be concerned with presenting some numerical examples of the propagation constants and EM field patterns that result when the theory which has been described in Section II is applied to the case of propagation in a four wire anechoic chamber. As a specific example a four wire anechoic chamber which has transverse dimension of $a = 1$ m and $b = 1$ m, a wire position of $x_o = .56$ m and $y_o = .62$ m, a wire radius of $\rho = .02$ m, which is covered by pyramidal absorbers which have a height of .2 m and is operated at a frequency of 47.7 MHz ($k_0 = 1.\mathrm{m}^{-1}$) has been chosen for study. Because of symmetry only the upper right quadrant of the insert of Fig. 1 need be analyzed. Propagation in this structure has been analyzed using the theory of Section II in conjunction with the variational expression presented in [9, Eq. 7.86, p. 347]. The modal expansion set used in the variational expression of [9] consisted of the TEM mode, the four

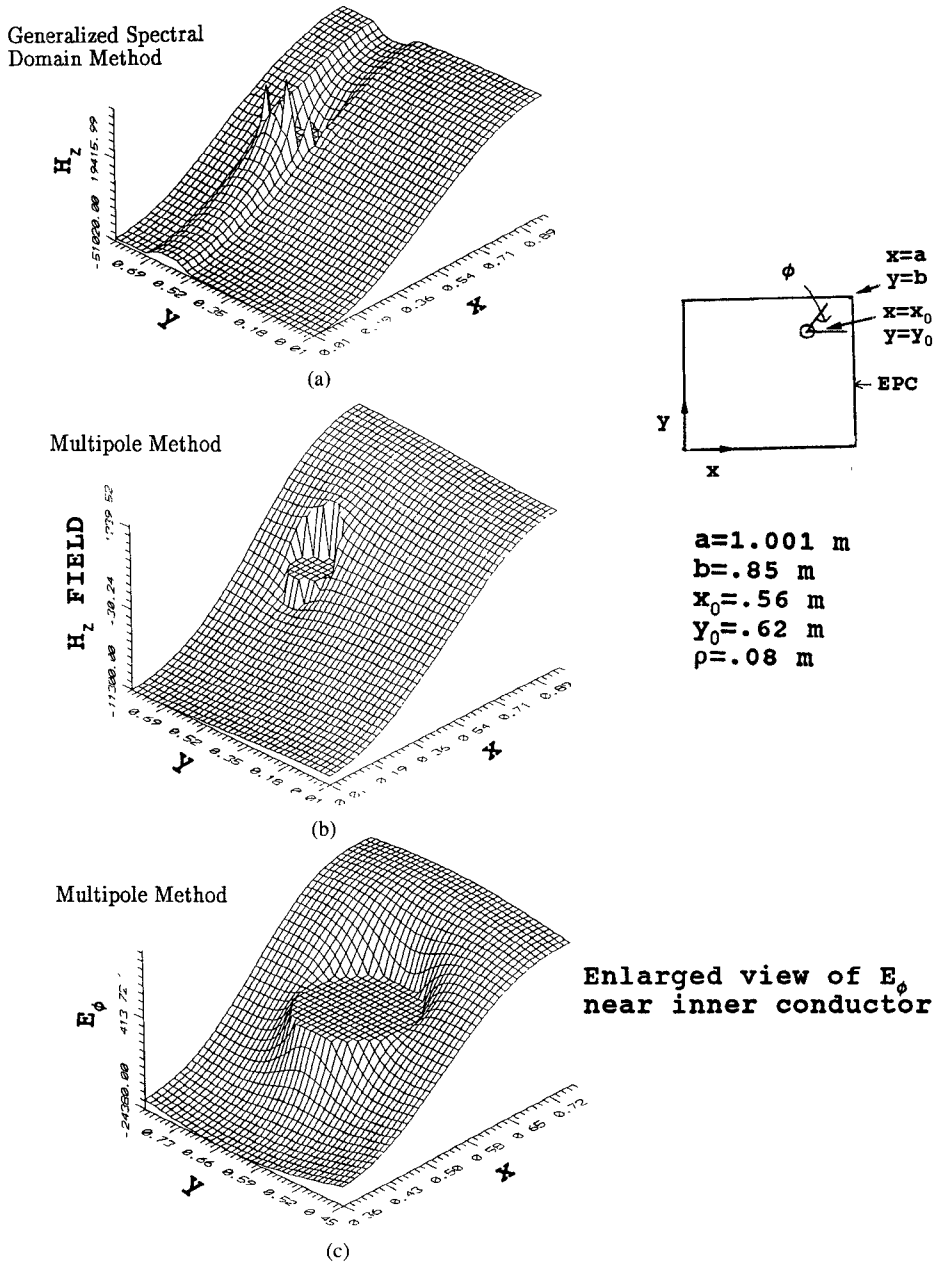

Fig. 4. (a) Shows the H_z field as results when the lowest order TE mode is determined in an off center, circular insert-rectangular waveguide using the GSD method and (b) shows the same mode as determined by the multipole method. (c) Shows the E_ϕ electric field as determined by the multipole method. The E_ϕ field is shown over a region .4 m by .4 m which is centered around the circular insert.

lowest order TE modes, and the four lowest order TM modes that could propagate in the non-dielectric filled coaxial waveguide. The non-dielectric filled coaxial waveguide in this case consists of 3 EPC walls and one MPC wall. The Fig. 1 caption gives the wall dielectric layer variation (see [8]) used in this section.

The four lowest TE modes in a coaxial rectangular waveguide were found to have cutoff wavenumbers of k_T = 1.57, 3.51, 4.70, and 5.66 m^{-1} and the four lowest TM modes were found to have cutoff wavenumbers of 3.88, 6.12, 6.76 and 8.16 (m^{-1}). Figs. 6(a) and (b) show respectively at cutoff, the E_z fields magnitude associated with first and fourth TM modes. This figure clearly shows the presence of the wire when calculating the TM eigenvalues of the system. The H_z field of the TE modes on the other hand was hardly perturbed by the presence of the wire. A numerical integration verified that the above modes were orthogonal to one another as they should be.

Fig. 7 shows the magnitude and phase of the E_y field as determined by the variational method of [9] when computed over the upper half of the cross section of the anechoic chamber (see Fig. 7 inset.) Three different dielectric cases were studied namely when the pyramidal relative dielectric permittivity assuming the values of $\epsilon_{rp} = 1 - j.1$, $2 - j.5$, and $3 - j1$. Fig. 7(a) shows the magnitude of E_y when $\epsilon_{rp} = 3 - j1$. The E_y magnitude varied little

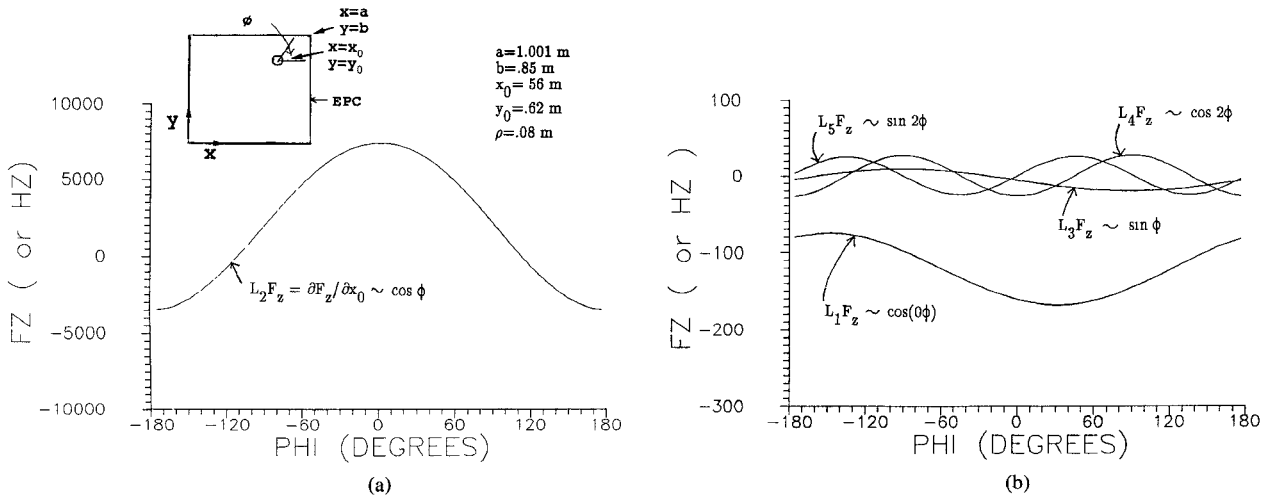

Fig. 5. (a) Shows a plot of the L_2F_z multipole contribution when evaluated at the circular insert surface as a function of ϕ. (b) Shows a plot of the other multipole terms. Each multipole in (a) and (b) has been multiplied by its corresponding a_l coefficient; $l = 1, \cdots, 5$ as determined by (9).

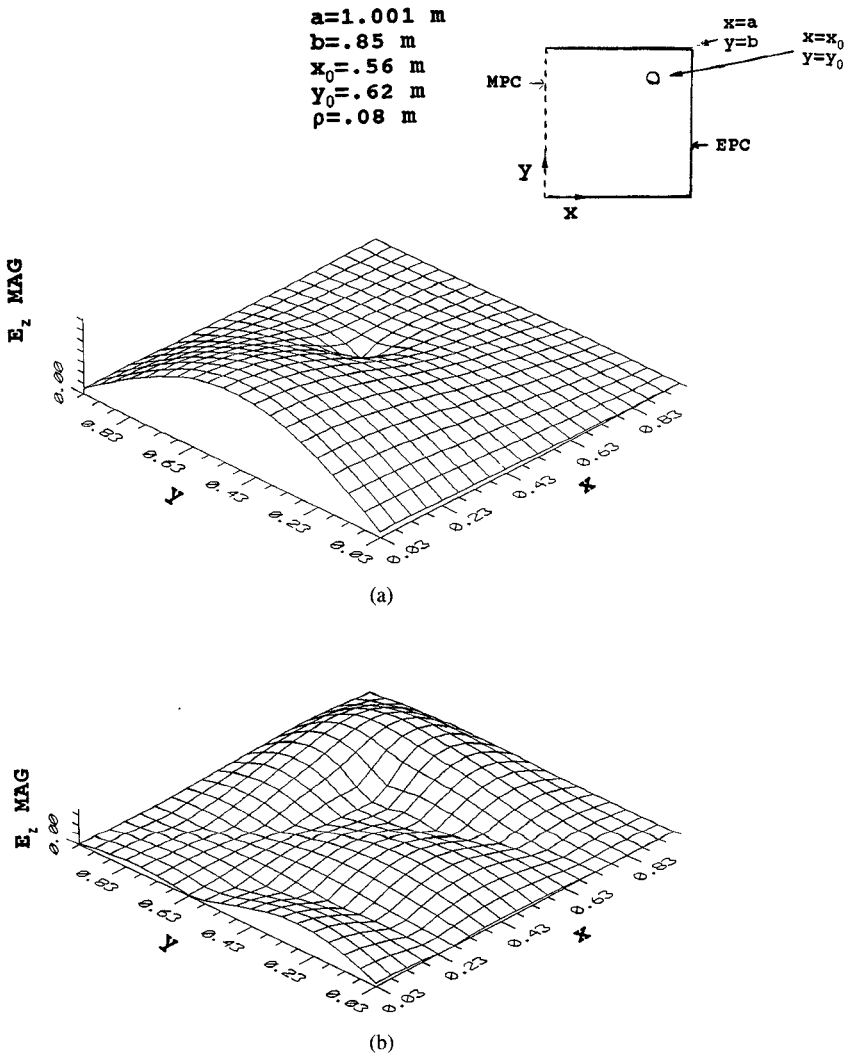

Fig. 6. The E_z electric field associated with the lowest order TM mode of rectangular waveguide of Fig. 2(b) is shown in (a) and the E_z electric field associated with the fourth lowest TM mode is shown in (b). These modes are used as expansion functions for the anechoic chamber.

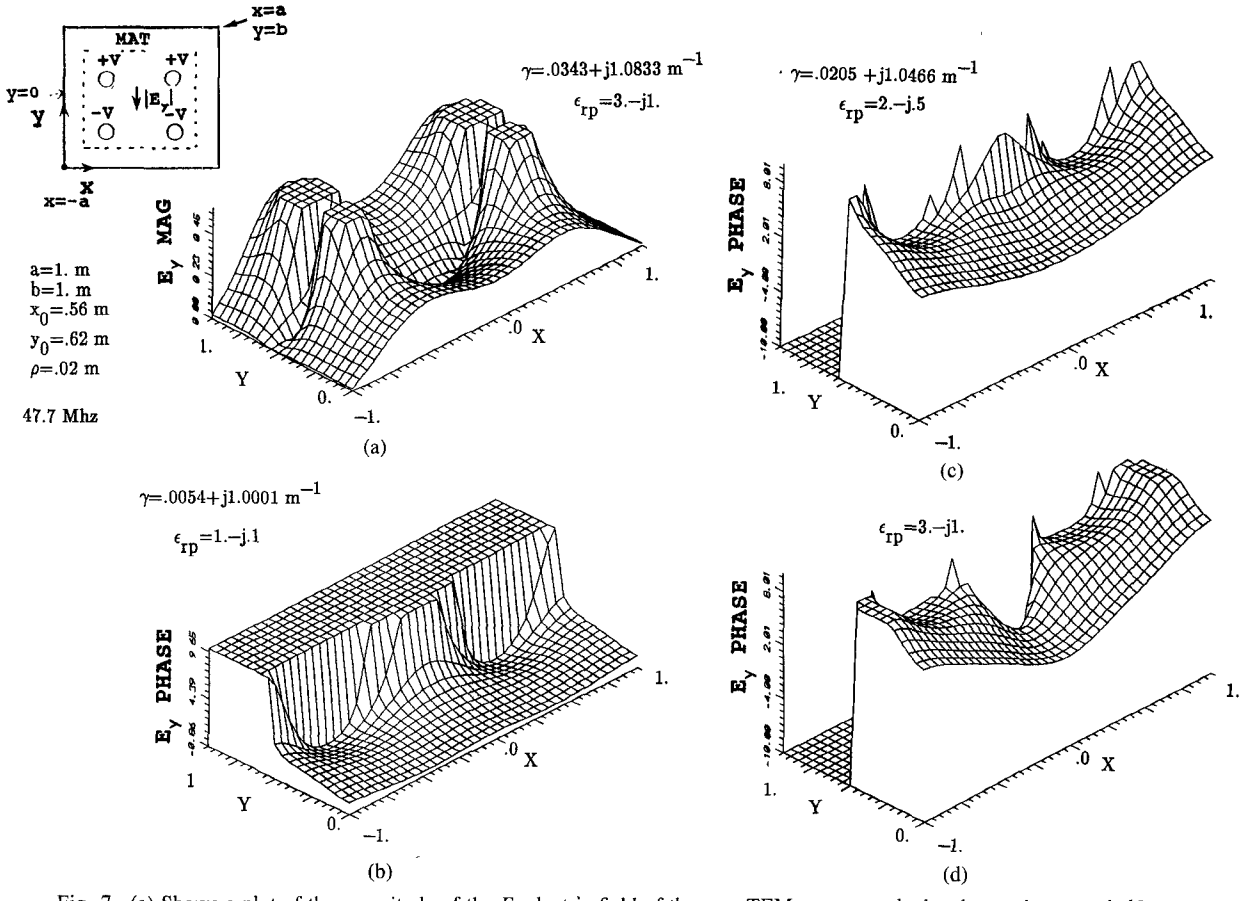

Fig. 7. (a) Shows a plot of the magnitude of the E_y electric field of the near TEM wave as calculated over the upper half cross section of the anechoic chamber shown in Fig. 1 (see inset.) (b)–(d) Show the phase (in degrees and referenced to the origin) of the E_y electric field.

with ϵ_{rp} and the magnitude of E_y was virtually the same for the other dielectric cases. Fig. 7(b), (c), and (d) show the phase of the E_y field when ϵ_{rp} was $1 - j.1$, $2 - j.5$, and $3 - j1$ respectively. As can be seen from these figures, ϵ_{rp} has a large effect on the uniformity of the phase of the E_y field as the real and imaginary part of ϵ_{rp} increase. In Fig. 7(b) when $\epsilon_{rp} = 1 - j.1$, the phase has a variation which is less than one degree over the target zone of the chamber, whereas in Fig. 7(c) and (d) the phase becomes increasingly bow shaped as the real and imaginary parts of ϵ_{rp} increase. The real and imaginary parts of the propagation constant were found to increase as the real and imaginary parts of ϵ_{rp} increased, as is physically expected. The propagation constant values are given on the figures.

In performing the matrix analysis of Fig. 6(a)–(d) it was found for a fixed value of ϵ_{rp} that the TE modes interacted very weakly with the near TEM mode of the system whereas the TM modes interacted strongly with this mode. In the dielectric loaded waveguide case, it was numerically verified that the complex modes satisfied z directed power orthogonality as is physically expected.

V. Summary and Conclusion

A generalized multipole analysis of the propagation in a circular insert loaded rectangular waveguide has been made when the coaxial waveguide was homogeneous and when the coaxial waveguide contained an inhomogeneous dielectric material. For the homogeneous waveguide case, the TE and TM eigenmodes of the system have been identified and field plots of them have been displayed. The higher order derivative multipoles were shown both theoretically and numerically to be close to sinusoids when evaluated close to the circular insert. Comparison of numerical results for the k_T of a centered circular insert with a ridged waveguide were shown to be in agreement. The L_2F_z multipole acting alone was found to provide an exact eigenvalue equation for a centered circular insert rectangular waveguide. Comparison of numerical results for the k_T of an off centered circular insert in a rectangular waveguide were made by the multipole method and the GSD method [5] and approximate agreement was found between the methods.

It is informative to compare the GSD method [5] with the multipole method of the present paper and of MW [1]. OS [5] have classified their method as a spectral domain method because of the fact that all EM fields and associated matrices elements that result from the application of their method can be expressed as an infinite summation over the sinusoidal waveguides modes which can propagate in an unloaded rectangular waveguide. The field amplitude expressions in the infinite summations which de-

pend on the modal wavenumbers $k_x = n\pi/a$, $k_y = m\pi/b$ ($n, m = 0, 1, 2, \cdots$) form the spectral representation of [5]. Using this classification criteria, the multipole method of the present paper and MW [1] can also be classified as a generalized spectral domain method since all field quantities depend on an infinite summation over the waveguide modes of the system. A chief difference which arises between the method of OS [5] and the multipole method of this paper is that the infinite series that arise in the multipole method converge much more rapidly than the series that arise in the OS [5] method. This is true because the GSD method of [5] involves a doubly infinite summation over products of sinusoidal functions and Bessel functions of the first kind (the Bessel functions arise from integration of the sinusoidal waveguide modes around the circular insert) which tend to go to zero slowly with increasing argument, whereas the multipole method used in the present paper (and MW [1]) involves only a singly infinite sum of products of sinusoids and decaying exponential terms. The decaying exponential terms go to zero rapidly with increasing argument. The present authors believe that rapid convergence of the series that occurs in the multipole method may be one of the reasons why Gibb's phenomena didn't arise in Figs. 4(b), 4(c), 5(a), and 5(b) using the multipole method, but did arise in Fig. 4(a) using the OS [5] method.

For the case when an inhomogeneous dielectric filled a wire loaded rectangular waveguide, the complex propagating modes were identified through the extremalization of a variational expression. EM field plots of the resulting propagation modes were given and it was shown that increasing phase distortion of the near TEM wave resulted as the real and imaginary parts of ϵ_r increased.

Appendix

In this appendix we apply the multipole method to the problem of determining the TM eigenmodes of a (inner conductor radius ρ) circular cylindrical coaxial waveguide when the wire is centered in the waveguide. According to this method we place an electric delta line current source at $r = 0$, and find the EM fields which arise from this source. Later these delta excited fields are point matched at the inner conductor surface to find the TM modes of the system.

To find the delta excited fields we solve the wave equation

$$\nabla^2 A_z + k^2 A_z = -I_o\, \delta(\vec{r})\, e^{-\gamma z} \tag{A1}$$

at cutoff $\gamma = 0$, and thus solve

$$\nabla_t^2 A_z + k_T^2 A_z = -I_o\, \delta(x)\, \delta(y) \tag{A2}$$

where $k_T = k$ is the unknown cutoff wavenumber (yet to be determined) of the coaxial circular waveguide. It is important to note that for any small but non zero value of ρ, k_T in (A2) is different in value than any of the cutoff frequencies of an unloaded or empty circular waveguide. (These are $k_{Tm,n}a = P_{m,n}$ where $P_{m,n}$ are roots of $J_n(P_{m,n}) = 0$). Because k_T is different from $k_{Tm,n}$, this means that the solution to (A2) is only the forced response due to $I_o\, \delta(\vec{r}_t)$ alone and that a separate homogeneous nonzero eigensolution A_z^e cannot also contribute to the A_z solution. Put another way, when $I_o = 0$, this implies $A_z = 0$.

To solve (A2) we surround the source $\delta(\vec{r}_t)$ by a loop of radius $\epsilon(\epsilon \to 0)$, find a homogeneous solution to (A2) exterior to the loop, and then apply Stokes' Theorem to Maxwell's second curl equation over the small loop to find the connection of the delta excitation with the homogeneous solution. The A_z solution exterior to the delta source after imposing boundary conditions ($A_z|_{r=a} = 0$) is given by

$$A_z = \sum_{n=-\infty}^{\infty} A_n [J_n(k_T r) + \beta_n N_n(k_T r)] e^{jn\phi}$$

where

$$\beta_n = -\frac{J_n(k_T a)}{N_n(k_T a)} \qquad r \geq \epsilon \tag{A3}$$

Application of Stokes' Theorem over the small loop ϵ surrounding the source is given by the equation

$$\begin{aligned} &\int \nabla \times \vec{H} \cdot \hat{a}_z\, ds \\ &\quad = \int_0^{2\pi} H_\phi|_{r=\epsilon}\, \epsilon\, d\phi \\ &\quad = j\omega\epsilon_o \int_{S_\epsilon} \vec{E} \cdot \hat{a}_z\, ds + I_o \int_{S_\epsilon} \delta(\vec{r})\, ds \end{aligned} \tag{A4}$$

where

$$\begin{aligned} H_\phi|_{r=\epsilon} &= \left.\frac{\partial A_z}{\partial r}\right|_{r=\epsilon} \\ &= \sum_{n=-\infty}^{\infty} A_n k_T [J_n'(k_T\epsilon) + \beta_n N_n'(k_T\epsilon)] e^{jn\phi}. \end{aligned} \tag{A5}$$

The first integral on the right most side of (A4) is zero as $\epsilon \to 0$ (as E_z is finite at the delta source) and the integral over delta function is unity. Integration from 0 to 2π over the infinite series gives zero for all terms except $n = 0$. Keeping only the $n = 0$ term, letting $\epsilon \to 0$ and using the small argument form of $N_o'(k_T\epsilon)$, we find $A_o = I_o/(4\beta_o)$ and that

$$\begin{aligned} A_z = \frac{I_o}{4J_o(k_T a)} &[J_o(k_T r)\, N_o(k_T a) \\ &- J_o(k_T a)\, N_o(k_T r)]. \end{aligned} \tag{A6}$$

Point matching $A_z(r)$ to zero at $r = \rho$ we find

$$0 = J_o(k_T\rho)\, N_o(k_T a) - J_o(k_T a)\, N_o(k_T\rho). \tag{A7}$$

This is the usual ϕ-independent (or $n = 0$) eigenvalue equation of a coaxial circular waveguide.

Note that when using the forced response of a single monopole that an azimuthally varying eigensolution such

as $[A_n(J_n(k_T r) + \beta_n N_n(k_T r)]e^{jn\phi}$, $n \neq 0$, cannot be determined from (A7).

An analysis of the TE equation

$$\nabla^2 F_z + k_T^2 F_z = -K_o\, \delta(\vec{r}) \tag{A8}$$

by a method similar to that used for (A2) shows the E_ϕ field is given by

$$E_\phi = \frac{K_o k_T}{4\beta_o'} [J_o'(k_T r) + \beta_o' N_o'(k_T r)] \tag{A9}$$

where

$$\beta_o' = -\frac{J_o'(k_T a)}{N_o'(k_T a)}.$$

Point matching of E_ϕ at $r = \rho$ shows the TE eigenequation is

$$0 = J_o'(k_T \rho)\, N_o'(k_T a) - J_o'(k_T a)\, N_o'(k_T \rho) \tag{A10}$$

which is the usual TE coaxial eigenvalue equation. It's interesting to note in this case that the use of a single magnetic monopole to solve (A8) doesn't predict the lowest order TE mode of coaxial circular waveguide regardless of how small the inner conductor radius is. (The lowest order coaxial waveguide mode approaches, for ρ small, the TE_{11} mode of a circular waveguide, namely, $E_z = J_1(k_T r) \sin \phi$). Use of a single monopole in a circular coaxial waveguide would lead to the conclusion that only ϕ symmetric solutions can exist in the waveguide.

The present authors believe that just as a circular coaxial waveguide can possess modes with ϕ variation close to the coaxial center conductor (even if its radius is small) that a conductor insert in a rectangular waveguide can also have modes which exhibit a ϕ variation close to the surface of the inner conductor. The present authors also believe that these modes cannot be formed by using a single ϕ-independent monopole, but require higher order multipoles (as given in [9]) for these modes proper determination.

In this appendix we would also like to see if a TE_{11} mode which has ϕ dependence ($\sin \phi$) and which cannot be determined by a single monopole, can have its eigenvalues determined by a multipole analysis. The multipole analysis in this case will consist of exciting the wave equation with a dipole source, rather than monopole source, calculating its E_ϕ field, and setting its E_ϕ to zero at the wire radius ρ. The dipole excited wave equation is

$$\nabla_t^2 F_z + k_T^2 F_z = -\frac{K_1}{r}\, \delta(r - r_o) \cdot \left[\delta\left(\phi - \frac{\pi}{2}\right) - \delta\left(\phi + \frac{\pi}{2}\right)\right] \tag{A11}$$

The solution of F_z in the above equation may be found by determining the delta response of a monopole located in a circular waveguide at a general point r_o, ϕ_o, specializing those results to the individual monopole responses of the monopoles in (A11) and then using superposition to add these responses together to get the response of (A11). The procedure used by James [15] can be used to find the response of (A11). Once the F_z solution is found, the E_ϕ solution is given by $E_\phi = \partial F_z / \partial \rho$. After performing algebra the E_ϕ solution is given by

$$E_\phi = \sum_{n=1}^{\infty} K_1 \left[\frac{J_n(k_T r_o)}{J_n'(k_T a)}\right]\left(\sin \frac{\pi}{2} n\right)(k_T) \cdot [N_n'(k_T a)\, J_n(k_T r) - J_n'(k_T a)\, N_n'(k_T r)] \sin n\phi \qquad r > r_o. \tag{A12}$$

As $r_o \to 0$, the $n = 1$ term is the dominant term of the series and thus only this term is retained. Setting $E_\phi = 0$ at $r = \rho$, we find

$$0 = N_1'(k_T a)\, J_1'(k_T \rho) - J_1'(k_T a)\, N_1'(k_T \rho)$$

which is the well known $n = 1$ TE eigenvalue equation for a coaxial circular waveguide.

A higher order derivative multipole solution does lead to ϕ dependent solution around the wire (in fact the exact eigenvalue equation in this case).

Acknowledgment

The authors of this paper would like to thank the reviewers for their detailed comments which greatly helped in the revision of this paper. The present authors would also like to thank V. Liepa, V. Maples, and J. Cole for their helpful comments concerning the four wire anechoic chamber.

References

[1] S. F. Mahmoud, and J. R. Wait, "Theory of wave propagation along a thin wire inside a rectangular waveguide," *Radio Science*, vol. 9, no. 3, pp. 417–420, Mar. 1974.

[2] T. K. Sarkar, K. Athar, E. Arvas, M. Manela, and R. Lade, "Computation of the propagation characteristics of TE and TM modes in arbitrarily shaped hollow waveguides utilizing the conjugate gradient method," *J. Electromagnetic Waves and Applications*, vol. 3, no. 2, 143–165, 1989.

[3] L. Gruner, "Higher order modes in rectangular coaxial waveguides," *IEEE Microwave Theory Tech.*, (Corresp.), vol. MTT-15, 483–485, Aug. 1967.

[4] W. Heinrich, "Full-wave analysis of conductor losses on MMIC transmission lines," *IEEE Trans. Microwave Theory Tech.*, vol. 38, no. 10, pp. 1468–1472, Oct. 1990.

[5] A. S. Omar, and K. F. Schünemann, "Application of the generalized spectral-domain technique to the analysis of rectangular waveguides with rectangular and circular inserts," *IEEE Trans. Microwave Theory Tech.*, vol. 39, no. 6, pp. 944–952, June 1991.

[6] —, "Analysis of waveguides with metal inserts," *IEEE Trans. Microwave Theory and Tech.*, vol. 37, pp. 1924–1932, 1989.

[7] V. V. Liepa and C. Cheon, "Analysis and design of 4-wire antenna for anechoic chamber excitation," in *1989 IEEE Antennas Propagat. Soc. Symp. Dig.*, vol. I, June 26, 1989, pp. 336–338.

[8] J. M. Jarem, "Electromagnetic field analysis of a four-wire anechoic chamber," *IEEE Trans. Antennas Propagat.*, vol. 38, no. 11, pp. 1835–1842, Nov. 1990.

[9] R. F. Harrington, *Time-Harmonic Electromagnetic Fields*. New York: McGraw-Hill, 1961.

[10] G. E. Bridges, "Interface effects on the propagation constant and fields of a bare conductor buried in a lossy half-space," in *1990 Antennas and Propagation Symp. Dig.*, Dallas, TX, May 7–11, pp. 332–335.

[11] R. J. Pogorzelski and D. C. Chang, "On the validity of the thin

approximation in analysis of wave propagation along a wire over a ground," *Radio Science*, vol. 12, pp. 699–707, 1977.
[12] C. Hafner, *The Generalized Multipole Technique for Computational Electromagnetics*. Norwood, MA: Artech House, 1990.
[13] J. D. Jackson, *Classical Electrodynamics*. New York: Wiley, 1962.
[14] R. E. Collin, *Field Theory of Guided Waves*. New York: McGraw-Hill, 1960, pp. 262–264.
[15] G. L. James, *Geometrical Theory of Diffraction for Electromagnetic Waves*, 3rd edition revised. London: Peregrinus, 1986, pp. 66–68.
[16] Y. Utsumi, "Variational analysis of ridged waveguide modes," *IEEE Trans. Microwave Theory Tech.*, vol. 33, no. 2, pp. 111–120, Feb. 1985.

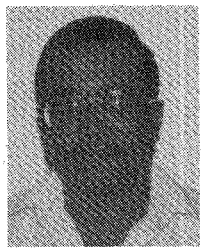

Magdy Z. Mohamed was born in Cairo, Egypt, on August 5, 1952. He received the B.S. degree in electrical and optical engineering from the Military Technical College, Cairo, Egypt, in 1975, and the M.S. degree in electronics from the College of Engineering, Cairo University, Egypt, in 1986. Since 1989, he has been working towards the Ph.D. degree in electrical engineering at the University of Alabama in Huntsville, where he is engaged in theoretical investigation and numerical analysis of wave propagation in inhomogeneous structures.

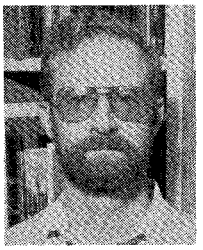

John M. Jarem (M'82) was born in Monterey, CA, on May 10, 1948. He received the B.S., M.S., and Ph.D. degrees in electrical engineering from Drexel University, Philadelphia, PA, in 1971, 1972, and 1975, respectively.

From 1975–1981 he worked as an Assistant Professor of Electrical Engineering at the University of Petrolem and Minerals in Dhahran, Saudia Arabia. He worked for the University of Texas at El Paso, as an Associate Professor of Electrical Engineering from 1981–1987 and has been a Professor of Electrical Engineering at the University of Alabama in Huntsville since 1987. His research interests are microwave theory, electromagnetics, and antenna theory.